Nuclear Instruments and Methods in Physics Research A285 (1989) 122–127
North-Holland, Amsterdam

GAIN REDUCTION IN FELS DUE TO DIFFRACTION LOSSES

Amnon FRUCHTMAN

Physics Department, Weizmann Institute of Science, 76100 Rehovot, Israel

The asymptotic expressions for the gain in the free electron lasers (FELs), which operate in the strong-pump Compton regime and in the collective Raman regime, and which employ a sheet electron beam and a cylindrical electron beam, are presented. For each case we identify a coupling parameter that measures the strength of the interaction. Large values of the coupling parameter correspond to strong optical guiding, while small values correspond to large diffraction. When the coupling parameter is small, the scaling of the gain is different from that of the one-dimensional theory because of diffraction losses. The particular scaling of the gain when diffraction losses are large depends both on the regime of operation and on the beam geometry. We give asymptotic expressions for the gain when diffraction is large for each case. This linear analysis is valid when the signal is small and is useful mainly when the gain is high prior to saturation.

1. Introduction

The modification of the transverse profile of the wave in the FEL and the associated optical guiding are subjects of extensive theoretical [1–14] and experimental [15–17] study. We examine these phenomena by formulating an eigenvalue problem for the transverse profile of the wave. The eigenfunctions are wave modes of a self-similar nature. They preserve their transverse profiles as they propagate. The imaginary part of the eigenvalue determines the growth rate of the mode.

The eigenvalue formulation is mostly useful to describe the interaction when the signal is small and the gain is high prior to saturation. It was applied to the FEL first by Moore [2] and later by others [3–5,10–14]. Moore analyzed a cylindrical electron beam FEL in the strong-pump regime, and identified a coupling parameter that measures the strength of the interaction. We extended Moore's analysis to the sheet beam FEL in the strong-pump regime [12], and to the cylindrical beam FEL in the collective Raman regime [14]. In this paper we study the sheet beam FEL in the collective Raman regime, and compare these four cases: the two different geometries and two different regimes of operation. We show that the coupling parameter and the scaling of the gain are different in each case. Strong optical guiding occurs when the coupling parameter is large, and diffraction is large when this coupling parameter is small. When the coupling parameter is large, the gain scales as it does in the 1-D (one-dimensional) theory. The reduction of the beam transverse dimensions (while the current is kept constant) increases the density, and, as a result, also the gain. However, if the coupling parameter is small, this reduction of beam transverse dimensions has also an opposite effect: it reduces the filling factor, increases diffraction losses, and, as a result, decreases the gain. Which of these opposing effects (the density increase or the filling factor decrease) is dominant depends on the geometry and on the regime of operation. In the cylindrical beam FEL in the strong-pump regime, for example, the gain keeps increasing if one uses a smaller radius beam, while in the Raman regime at small radii the gain decreases when the radius is reduced.

In section 2 we write expressions for the transverse wave profile and for the gain in the sheet beam FEL in the Raman regime. We derive asymptotic expressions for the profile and gain when the coupling parameter takes large and small values. We also use an energy integral method to locate the nonreal eigenvalues. In section 3 we compare the FEL interaction in the different geometries and different regimes of operation. We conclude in section 4 by discussing the validity of our results.

2. The sheet beam FEL in the collective Raman regime

We analyze an FEL with a sheet electron beam, which is infinitely wide in the x-direction, of width $2a$ in the y-direction, and which propagates in the z-direction along a planar magnetic wiggler field of the form

$$\boldsymbol{B}_0 = \hat{e}_y B_w \sin(k_w z). \tag{1}$$

Operation of an FEL which employs a sheet electron beam has recently been reported [18]. The governing equation was shown by us to be [13]

$$\frac{\partial^2 \delta E_x}{\partial \bar{y}^2} + \left\{ \phi^2 + \frac{\alpha_{sh}^R}{\left[\phi^2 - \zeta - f(\bar{y})\right]} \right\} \delta E_x = 0, \tag{2a}$$

0168-9002/89/$03.50

for $|\bar{y}| < 1$ and

$$\frac{\partial^2 \delta E_x}{\partial \bar{y}^2} + \phi^2 \delta E_x = 0, \tag{2b}$$

for $|\bar{y}| > 1$. The coupling parameter α_{sh}^R in the Raman regime and sheet electron beam is

$$\alpha_{sh}^R \equiv 8k_w^3 (\omega_p/c) a_w^2 \gamma^{5/2} a^4, \tag{3a}$$

or equivalently

$$\alpha_{sh}^R = \sqrt{\frac{2}{c}}\, 4k_w^3 J^{1/2} a_w^2 \gamma^{5/2} a^{7/2}, \tag{3b}$$

where

$$J \equiv 2a\left(\frac{\omega_p^2}{c^2}\right) v_z$$

is the normalized current. The normalized eigenvalue is

$$\phi^2 \equiv -2\frac{\omega}{c} a^2 \left(k_z - \frac{\omega}{c}\right), \tag{4}$$

and the normalized detuning (mismatch) parameter is

$$\zeta \equiv 2\frac{\omega}{c} a^2 \left[\frac{\omega}{c}\left(1 - \frac{c}{v_z}\right) + k_w - \frac{\omega_p}{v_z \gamma^{3/2}} \left(1 + a_w^2\right)^{1/2}\right]. \tag{5}$$

Here ω and k_z are the wave frequency and wave number, ω_p is the beam plasma frequency, $\gamma = (1 - v^2/c^2)^{-1/2}$ is the beam energy and v its velocity. In writing the expression for α_{sh}^R we assumed that $k_z \cong \omega/c \cong 2k_w\gamma^2$, that $v_z \cong c$, and that $a_w^2 \ll 1$. Also, the beam is assumed to be cold. We allow a small transverse density gradient

$$\omega_p^2 = \omega_{p0}^2 + \omega_{p1}^2(y), \quad |y| \le a, \tag{6}$$

where

$$\omega_{p1}^2(y) \ll \omega_{p0}^2, \tag{7}$$

and $\omega_p^2 = 0$, when $|y| > a$. In eq. (3a) $\omega_p^2 = \omega_{p0}^2$. The density variation is expressed through $f(\bar{y})$, where

$$f(\bar{y}) = -\frac{\omega}{c}\frac{a^2}{\omega_{p0}} \frac{\left(1 + a_w^2\right)^{1/2}}{v_z \gamma^{3/2}} \omega_{p1}^2(\bar{y}). \tag{8}$$

The wiggler parameter a_w is $eB_w/(\sqrt{2}\, mc^2 k_w)$, where e and m are the electron charge and mass. The normalized coordinate is $\bar{y} \equiv y/a$. We apply an energy integral method to locate the nonreal eigenvalues, similarly to what we did in the analysis of the cylindrical beam [14].

We limit ourselves to symmetrical density profiles, $f(\bar{y}) = f(-\bar{y})$, and look for symmetrical solutions, $\delta E_x(\bar{y}) = \delta E_x(-\bar{y})$. We therefore require

$$\frac{\partial \delta E_x(0)}{\partial \bar{y}} = 0, \tag{9}$$

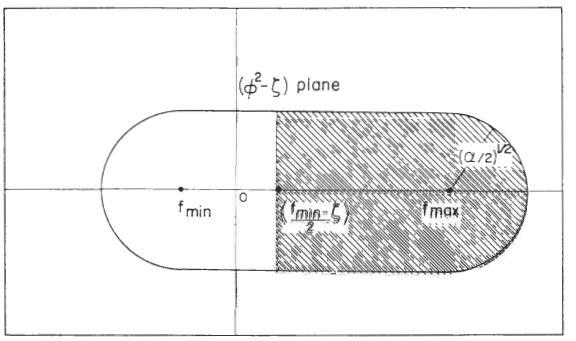

Fig. 1. The domain in the complex $(\phi^2 - \zeta)$ plane where nonreal eigenvalues are allowed.

and solve for $\bar{y} \in [0, \infty)$. When no waveguide is present, the solution for $\bar{y} \ge 1$ is

$$\delta E_x = b\, e^{i\phi\bar{y}}, \ \mathrm{Im}\ \phi > 0. \tag{10}$$

We multiply the equation by δE_x^* and integrate from zero to infinity. Using eqs. (9) and (10) we obtain

$$-\int_0^1 d\bar{y} \left|\frac{\partial \delta E_x}{\partial \bar{y}}\right|^2 + \int_0^1 d\bar{y}\, |\delta E_x|^2 \left\{\phi^2 + \frac{\alpha_{sh}^R \left[\phi^{2*} - \zeta + f(\bar{y})\right]}{|\phi^2 - \xi - f(\bar{y})|^2}\right\} = 0. \tag{11}$$

We first take the imaginary part of eq. (11). If $\mathrm{Im}(\phi^2) \neq 0$, we get

$$\int_0^1 d\bar{y}\, |\delta E_x|^2 \left\{1 - \frac{\alpha_{sh}^R}{|\phi^2 - \zeta - f(\bar{y})|^2}\right\} = 0. \tag{12}$$

The term in the braces has to take both positive and negative values. There must be $\bar{y} \in [0, 1]$ where

$$\frac{\alpha_{sh}^R}{|\phi^2 - \zeta - f(\bar{y})|^2} > 1. \tag{13}$$

The nonreal eigenvalues are allowed in the domain of the stadium shape shown in fig. 1. Taking the real part of eq. (11) and using the negativity of the first term, we find that

$$\int_0^1 d\bar{y}\, |\delta E_x|^2 \left\{\mathrm{Re}(\phi^2) + \frac{\alpha_{sh}^R \left[\mathrm{Re}(\phi^2) - \zeta - f(\bar{y})\right]}{|\phi^2 - \zeta - f(\bar{y})|^2}\right\} > 0. \tag{14}$$

We multiply eq. (12) by $\mathrm{Re}(\phi^2)$ and subtract it from eq. (14). We obtain

$$\int_0^1 d\bar{y}\, |\delta E_x|^2 \left\{\frac{2\,\mathrm{Re}(\phi^2) - \zeta - f(\bar{y})}{|\phi^2 - \zeta - f(\bar{y})|^2}\right\} > 0. \tag{15}$$

Again, the term in the braces has to take a positive value for some $\bar{y}$. Therefore

$$\mathrm{Re}\ \phi^2 - \zeta > \frac{(f_{\min} - \zeta)}{2}. \tag{16}$$

The shaded area in fig. 1 represents the domain in the complex $(\phi^2$–$\zeta)$ plane, where both inequalities (13) and (16) are satisfied, and where, therefore, nonreal eigenvalues are allowed. In order that nonreal eigenvalues be allowed, the detuning parameter has to satisfy the inequality

$$\zeta > -2\left(\alpha_{\mathrm{sh}}^{\mathrm{R}}\right)^{1/2} - 2f_{\max} + f_{\min}. \tag{17}$$

Having determined the domain in the complex plane where nonreal eigenvalues are allowed, we turn now to the gain and the transverse wave profile. The reduction of gain due to density nonuniformities, especially for the case of large f, has been analyzed by Fruchtman and Weitzner [13]. In the following we assume that the density is uniform,

$$\omega_{\mathrm{p1}}^2 = 0. \tag{18}$$

Eq. (2a) takes the simpler form

$$\frac{\partial^2 \delta E_x}{\partial \bar{y}^2} + \left[\phi^2 + \frac{\alpha_{\mathrm{sh}}^{\mathrm{R}}}{(\phi^2 - \zeta)}\right]\delta E_x = 0. \tag{19}$$

For notational convenience we denote $\alpha_{\mathrm{sh}}^{\mathrm{R}}$ as α in the rest of this section. The analysis is equivalent to our analysis of the sheet-beam FEL in the strong-pump regime [12]. We first assume that a conductor is located at $\bar{y} = 1$, and require that

$$\delta E_x(1) = 0. \tag{20}$$

The solution of eq. (19), subject to the boundary condition (9), is thus

$$\delta E_x = \cos(\chi \bar{y}), \tag{21}$$

where

$$\chi^2 \equiv \phi^2 + \frac{\alpha}{(\phi^2 - \zeta)}. \tag{22}$$

As a result of condition (20), we obtain

$$\chi^2 = \left(\frac{\pi}{2}\right)^2 (2n+1)^2, \qquad n = 0, 1, 2, \ldots. \tag{23}$$

For each α and ζ there is an infinite set of eigenvalues which satisfy

$$(\phi_n^2 - \zeta)\left[\phi_n^2 - \left(\frac{\pi}{2}\right)^2 (2n+1)^2\right] + \alpha = 0. \tag{24}$$

If

$$\left[\zeta - \left(\frac{\pi}{2}\right)^2 (2n+1)^2\right]^2 < 4\alpha, \tag{25}$$

the two roots of eq. (24) become nonreal. When

$$\zeta = \left(\frac{\pi}{2}\right)^2 (2n+1)^2 \tag{26}$$

the eigenvalue has its maximal imaginary part

$$\mathrm{Im}\ \phi_n^2 = \alpha^{1/2}, \tag{27}$$

which is the same as in the 1-D case.

Let us assume now that n is large so that

$$\left(\frac{\pi}{2}\right)^2 (2n+1)^2 \ll \zeta,\ 2\alpha^{1/2}. \tag{28}$$

In that case, following (25), the instability vanishes. One of the eigenvalues which corresponds to the eigenfunction

$$\delta E_x = \cos\left[\left(\frac{\pi}{2}\right)(2n+1)\,\bar{y}\right] \tag{29}$$

is

$$\phi_{n,1}^2 \cong \left(\frac{\pi}{2}\right)^2 (2n+1)^2 - \frac{\alpha}{\left(\frac{\pi}{2}\right)^2 (2n+1)^2}, \tag{30}$$

and is close to the vacuum solution. The second eigenvalue that corresponds to the eigenfunction (29) is

$$\phi_{n,2}^2 \cong \zeta - \frac{(\zeta^2 - 4)\alpha}{4\left(\frac{\pi}{2}\right)^2 (2n+1)^2}. \tag{31}$$

Thus ζ is an accumulation point of real eigenvalues. This is different from the case of the strong-pump regime [12] where there was an accumulation point of unstable modes.

We turn now to the case in which no waveguide is present. The boundary conditions at $\bar{y} = 1$ are now the continuity of the wave and its derivative. The wave fields (10) and (29) and their derivatives are equal at $\bar{y} = 1$. Thus, the dispersion relation is

$$\frac{\chi(e^{i\chi} - e^{-i\chi})}{(e^{i\chi} + e^{-i\chi})} = \phi. \tag{32}$$

We look now for solutions of the dispersion relation for large and for small values of the coupling parameter α. When α is large, ϕ is expected to be larger than χ, and thus to lowest order

$$e^{i\chi} + e^{-i\chi} = 0, \tag{33}$$

and

$$\chi_0 = \frac{\pi(2n+1)}{2}. \tag{34}$$

The eigenvalue is

$$\phi_0^2 = i\alpha^{1/2}, \tag{35}$$

as in the 1-D theory. The wave profile inside the beam is the same as in the case of a guided wave. This is the case of strong optical guiding. In order to obtain the

form of the wave outside the electron beam we solve the equations to the next order. The dispersion relation to the next order yields

$$\chi_0 = \mathrm{i}\phi_0\chi_1 \tag{36}$$

and

$$b_0 = -2\chi_1\, \mathrm{e}^{-\mathrm{i}\phi_0} \tag{37}$$

Thus, for large α, the wave is

$$\delta E_x = 2\cos\left\{\left(\frac{\pi}{2}\right)(2n+1)\left[1-\frac{1+\mathrm{i}}{\sqrt{2}\,\alpha^{1/4}}\right]\bar{y}\right\}, \quad \bar{y}\le 1;$$

$$\delta E_x = \frac{(2n+1)\pi}{\alpha^{1/4}}\exp\left\{\mathrm{i}\pi/4+(-1+\mathrm{i})\frac{\alpha^{1/4}}{\sqrt{2}}(\bar{y}-1)\right\},$$

$$\bar{y}\ge 1. \tag{38}$$

In this case of strong optical guiding the wave is confined to the electron beam and decays fast to zero at the beam transverse edge.

When α is small, the eigenvalue ϕ^2 is expected to be smaller than χ^2. To lowest order we have

$$\mathrm{e}^{\mathrm{i}\chi} - \mathrm{e}^{-\mathrm{i}\chi} = 0, \tag{39}$$

and also

$$\chi^2 = \frac{\alpha}{(\phi^2-\zeta)}. \tag{40}$$

Thus

$$\chi_0 = n\pi, \tag{41}$$

and

$$\phi_0^2 = \zeta + \frac{\alpha}{n^2\pi^2}, \tag{42}$$

where we assume that ζ is much smaller than 1, and that n is not zero. When χ is smaller than 1, we obtain from eq. (32) to lowest order, instead of eq. (41),

$$\mathrm{i}\chi_0^2 = \phi_0. \tag{43}$$

Together with eq. (40), this yields

$$\phi(\phi^2-\zeta) = \mathrm{i}\alpha. \tag{44}$$

For $\zeta = 0$, the eigenvalue becomes

$$\phi^2 = \mathrm{e}^{\mathrm{i}\pi/3}\alpha^{2/3}. \tag{45}$$

Only the fundamental solution is unstable for small α, and the growth rate scales as $\alpha^{2/3}$ and not as $\alpha^{1/2}$ (as it does in the 1-D case). The reduction in the growth rate originates from the reduction in the filling factor. Indeed, when α is small, the solution exhibits a large diffraction. Its form is

$$\delta E_x = 1 + \mathrm{e}^{\mathrm{i}2\pi/3}\alpha^{1/3}\bar{y}^2/2, \qquad \bar{y}\le 1,$$

$$\delta E_x = \left[1-\left(\frac{-1+\mathrm{i}\sqrt{3}}{2}\right)\alpha^{1/3}/2\right]$$

$$\times\exp\left[\left(\frac{-1+\mathrm{i}\sqrt{3}}{2}\right)\alpha^{1/3}\bar{y}\right], \qquad \bar{y}\ge 1. \tag{46}$$

We now write the gain for large and for small values of the coupling parameter in the original units

$$\mathrm{Im}\ k_z = -a_\mathrm{w}\left(\frac{\omega_\mathrm{p}^2 k_\mathrm{w}^2}{4\gamma^3 c^2}\right)^{1/4}$$

$$= -a_\mathrm{w}\left(\frac{Jk_\mathrm{w}^2}{8\gamma^3 ca}\right)^{1/4}, \qquad \alpha\gg 1; \tag{47a}$$

$$\mathrm{Im}\ k_z = -\frac{\sqrt{3}}{2}k_\mathrm{w}\left(\frac{a_\mathrm{w}^4\omega_\mathrm{p}^2 a^2}{\gamma c^2}\right)^{1/3}$$

$$= -\frac{\sqrt{3}}{2}k_\mathrm{w}\left(\frac{a_\mathrm{w}^4 Ja}{2\gamma c}\right)^{1/3}, \quad \alpha\ll 1. \tag{47b}$$

In the next section we compare the gain for the two geometries and for the two regimes of operation.

3. Comparison of various gains

In a previous paper [12] we identified the coupling parameter $\alpha_\mathrm{sh}^\mathrm{com}$ for a sheet beam FEL in the strong-pump Compton regime

$$\alpha_\mathrm{sh}^\mathrm{com} = 16k_\mathrm{w}^4\left(\omega_\mathrm{p}^2/c^2\right)a_\mathrm{w}^2\gamma^3 a^6, \tag{48a}$$

or equivalently

$$\alpha_\mathrm{sh}^\mathrm{com} = 8k_\mathrm{w}^4(J/c)a_\mathrm{w}^2\gamma^3 a^5. \tag{48b}$$

The gain was shown to be asymptotically

$$\mathrm{Im}\ k_z = -\frac{1}{2}\sqrt{\frac{3}{2}}\left(\frac{\omega_\mathrm{p}^2 k_\mathrm{w} a_\omega^2}{\gamma^3 v_z^2}\right)^{1/3}$$

$$= -\frac{1}{2}\sqrt{\frac{3}{2}}\left(\frac{Jc^2 k_\mathrm{w} a_\mathrm{w}^2}{2a\gamma^3 v_z^3}\right)^{1/3}, \qquad \alpha\gg 1; \tag{49a}$$

and

$$\mathrm{Im}\ k_z = -\tfrac{1}{2}\sin\left(\frac{3\pi}{5}\right)\left(\frac{2\omega_\mathrm{p}^2 k_\mathrm{w} a_\mathrm{w}^2}{\gamma^3 v_z^2}\right)^{2/5}\left(\frac{\omega}{c}\right)^{1/5}a^{2/5}$$

$$= -\tfrac{1}{2}\sin\left(\frac{3\pi}{5}\right)\left(\frac{Jc^2 k_\mathrm{w} a_\mathrm{w}^2}{\gamma^3 v_z^3}\right)^{2/5}\left(\frac{\omega}{c}\right)^{1/5},$$

$$\alpha\ll 1. \tag{49b}$$

where $J = 2(\omega_\mathrm{p}^2/c^2)v_z a$.

We note that the effect of diffraction on the gain is different for the two regimes of operation. In both regimes, when α is large, if the current J is kept constant while a is reduced, the gain increases because of the density increase, as it does in the 1-D case. When α is small, however, this reduction of a is followed also by a reduction of the filling factor, by diffraction losses, and as a result, by a decrease in gain. The relative roles of the density increase and filling factor decrease are

different for the two different regimes. In the Compton regime these two opposing effects compensate each other when α is small and the gain is independent of a. In the Raman regime, the filling factor decrease is dominant when α is small and the gain decreases when a is reduced. Thus, the scaling of the gain with a is nonmonotonic in the Raman regime. When α is large and a is reduced the gain increases. If a is reduced much further until α becomes small, the gain starts to decrease. Therefore, in the Raman regime, for a given current, there is an optimal thickness at which the gain is maximal.

The geometry affects the scaling of the gain as well. Moore studied the cylindrical beam FEL in the strong-pump Compton regime [2]. When a helical wiggler of the form

$$\boldsymbol{B}_w = B_w\left[\hat{e}_x \cos(k_w z) + \hat{e}_y \sin(k_w z)\right], \tag{50}$$

is employed, the coupling parameter is

$$\alpha_{\mathrm{cyl}}^{\mathrm{com}} = 32 k_w^4 \left(\omega_p^2/c^2\right) a_w^2 \gamma^3 r_b^6, \tag{51a}$$

or equivalently

$$\alpha_{\mathrm{cyl}}^{\mathrm{com}} = 32 k_w^4 \left(I/\pi c\right) a_w^2 \gamma^3 r_b^4, \tag{51b}$$

where the wiggler parameter here a_w is $eB_w/(mc^2 k_w)$, $I = (\omega_p^2/c^2)\pi r_b^2 c$, and r_b is the beam radius. These expressions, aside from numerical factors, are identical to those in eq. (48) for $\alpha_{\mathrm{sh}}^{\mathrm{com}}$. When α is large, the gain is as in the 1-D case. The asymptotic expressions for the gain are

$$\begin{aligned}\mathrm{Im}\ k_z &= -8\frac{\sqrt{3}}{2}\left[k_w^4\left(\omega_p^2/c^2\right)a_w^2\gamma^3\right]^{1/3} \\ &= -8\frac{\sqrt{3}}{2}\left(\frac{k_w^4 I a_w^2 \gamma^3}{\pi c r_b^2}\right)^{1/3}, \qquad \alpha \gg 1,\end{aligned} \tag{52a}$$

and

$$\begin{aligned}\mathrm{Im}\ k_z &= k_w\left(\omega_p^2/c^2\right)a_w\gamma^{3/2}r_b \\ &\quad\times\left\{-\ln\left[\sqrt{2}\,k_w\left(\omega_p/c\right)^{1/2}a_w^{1/2}\gamma^{3/4}r_b^{3/2}\right]\right\}^{1/2} \\ &= -k_w\left(I/\pi c\right)a_w\gamma^{3/2} \\ &\quad\times\left\{-\ln\left[\sqrt{2}\,k_w\left(I/\pi c\right)^{1/4}a_w^{1/2}\gamma^{3/4}r_b\right]\right\}^{1/2}, \\ &\alpha \ll 1.\end{aligned} \tag{52b}$$

As pointed out by Moore [2], if r_b is reduced while I is kept constant, the gain keeps increasing, even though the increase is very slow when α is small.

We studied the case of a cylindrical beam FEL in the Raman regime [14]. The coupling parameter was shown to be

$$\alpha_{\mathrm{cyl}}^{\mathrm{R}} = 4 k_w^3 \left(\omega_p/c\right) a_w^2 \gamma^{5/2} r_b^4, \tag{53a}$$

or equivalently

$$\alpha_{\mathrm{cyl}}^{\mathrm{R}} = 4 k_w^3 \left(I/\pi c\right)^{1/2} a_w^2 \gamma^{5/2} r_b^3. \tag{53b}$$

The asymptotic expressions for the gain were

$$\begin{aligned}\mathrm{Im}\ k_z &= -\frac{a_w}{2}\left[\frac{k_w\left(\omega_p/c\right)}{\gamma^{3/2}}\right]^{1/2} \\ &= -\frac{a_w}{2}\left[\frac{k_w\left(I/\pi c\right)^{1/2}}{\gamma^{3/2} r_b}\right]^{1/2}, \qquad \alpha \gg 1,\end{aligned} \tag{54a}$$

$$\begin{aligned}\mathrm{Im}\ k_z &= -\frac{\pi}{4}k_w^2\left(\omega_p/c\right)a_w^2\gamma^{1/2}r_b^2 \\ &= -\frac{k_w^2}{4}\left(\frac{I}{\pi c}\right)^{1/2}a_w^2\gamma^{1/2}r_b, \qquad \alpha \ll 1.\end{aligned} \tag{54b}$$

In the Raman regime in the cylindrical geometry, we again find a nonmonotonic dependence of the gain on the beam dimensions. For large α, the gain increases when r_b is reduced, while for small α, the gain decreases when r_b is reduced. When α is small, the diffraction losses are dominant in the Raman regime, while the density increase is dominant in the Compton regime.

4. Conclusions

In the previous sections we discussed the FEL interaction in two different geometries and two different regimes of operation. The interaction was characterized by the wiggler wavenumber k_w and intensity a_w, the beam density ω_p^2 and energy γ, and the beam transverse dimension (a or r_b). For each case a different combination of those parameters gave a coupling parameter that measures the strength of the interaction. We were able to give analytic expressions for the gain in limiting cases.

We emphasize that in practice one rarely encounters a situation where the asymptotic expressions are realized. The coupling parameter has to be very large or very small in order for these expressions to be valid, and in reality it is usually of order of one. If the coupling parameter is very small, the exponential growth may be too small to be measured. When the filling factor of the FEL eigenmodes is very small and they extend to a large distance transversely, elements of the experimental setup will perturb the profile of the eigenmodes and not allow them to evolve. Moreover, the two regimes of operation, the Compton and the Raman regimes, are not always distinct. Sometimes a system operates in an intermediate regime. Important effects such as beam emittance and thermal spread were not included in this analysis.

Despite the limitations on the validity of these asymptotic expressions, they are important since they exhibit the interplay between various physical mechanisms that are present in the FEL, as well as the relative roles of the gain mechanism and diffraction loss in various geometries and regimes of operation.

Acknowledgement

This work was supported by the Koret Foundation.

References

[1] E.T. Scharlemann, A.M. Sessler and J.S. Wurtele, Phys. Rev. Lett. 54 (1985) 1925.
[2] G.T. Moore, Nucl. Instr. and Meth. A239 (1985) 19.
[3] P. Luchini and S. Solimeno, Nucl. Instr. and Meth. A250 (1985) 413.
[4] M. Xie and D.A.G. Deacon, Nucl. Instr. and Meth. A250 (1985) 426.
[5] K.J. Kim, Phys. Rev. Lett. 57 (1986) 1871.
[6] B. Hafizi, P. Sprangle and A. Ting, Phys. Rev. A36 (1987) 1739.
[7] S.Y. Cai, A. Bhattacharjee and T.C. Marshall, IEEE J. Quantum Electron. QE-23 (1987) 1651.
[8] E. Jerby and A. Gover, Nucl. Instr. and Meth. A272 (1988) 380.
[9] H.P. Freund, H. Bluem and C.L. Chang, Nucl. Instr. and Meth. A272 (1988) 556.
[10] Li-Hua Yu and S. Krinsky, Phys. Lett. A129 (1988) 463.
[11] T.M. Antonsen Jr. and P.E. Latham, Phys. Fluids 32 (1988) 3379.
[12] A. Fruchtman, Phys. Rev. A37 (1988) 2989.
[13] A. Fruchtman and H. Weitzner, Phys. Rev. A39 (1989) 658.
[14] A. Fruchtman, submitted to Phys. Rev. A.
[15] R.W. Warren and B.D. McVey, Nucl. Instr. and Meth. A259 (1987) 154.
[16] F. Hartemann, K. Xu, G. Bekefi and J.S. Wurtele, Phys. Rev. Lett. 59 (1987) 1177.
[17] A. Bhattacharjee, S.Y. Cai, S.P. Chang, J.W. Dodd and T.C. Marshall, Phys. Rev. Lett. 60 (1988) 1254.
[18] V.L. Granatstein, T.M. Antonsen, Jr., J.H. Booske, W.W. Destler, P.E. Latham, B. Levush, I.D. Mayergoyz, D.J. Radack, Z. Segalov and A. Serbeto, Nucl. Instr. and Meth. A272 (1988) 110.